International Journal of Chemistry and Material Science Vol. 1(3), pp. 055-068, March 2013
Available online at http://www.academeresearchjournals.org/journal/ijcms
ISSN 2327-5553 ©2013 Academe Research Journals

Full Length Research Paper

Electrical conductivity measurements of mixed oxide catalysts used as a typical reaction of heavy water production

A. M. El-Sharkawy

Chemistry Department, Faculty of Science, Benha University, Egypt. E-mail: sashama92@yahoo.com.

Accepted 19 January, 2013

The alternative conductivity (AC) of nickel catalysts promoted with Fe_2O_3 and supported with Al_2O_3, CoO and MnO was examined using a conductivity bridge and applying the complex impedance method. The obtained semicircles permitted calculation of the electrical conductance for the examined samples. The results show that they have an electronic nature. The electrical properties of the catalysts depend on their structure and composition. Their resistance may be a combination of bulk crystal resistance and grain boundary one. The variation of conductivity with temperature for the examined catalytic systems shows an increase of resistance with decreasing temperature, indicating an activated conduction and semiconductor nature.

Key words: Conductimetric measurements, complex impedance plots, dielectric constant, activation energy, frequency and capacitance.

INTRODUCTION

The conductivity measurements of solid catalysts could be obtained through graphical dialysis of the obtained data resulting from the corresponding AC response. Graphical dialysis of the a.c. data could be expressed in four basic formalism (Smallman and Ngan, 2007; Moseley, 2009; Gouda and Nagendro, 2009). These are most conveniently expressed as:

a- The complex admittance; $Y^* = (R_p)^{-1} + JWC_p$ (1)

b- The complex impedance; $Z^* = (Y^*)^{-1} = R_s - \frac{J}{WCs}$ (2)

c- The complex permittivity; $\in^* = \in^{/} - Jc^{//}$ (3)

d- The complex modulus; $M^* = (\in^*)^{-1} = M^{/} + JM^{//}$ (4)

Where the subscripts p and s refer to the equivalent parallel and series circuit components, respectively.

These functions separate into two groups representing parallel and series formalism.
The two parallel or admittance functions are related:

$Y^* = JWC_o \in^*$ (5)

Similarly the series functions are related:

$M^* = JWC_o Z^*$ (6)

Where C_o is the vacuum capacitance of the cell.

The quantities Y^*, Z^* and $\in^*$ constitute standard textbook material. The principle of the complex impedance analysis given by Equation 2 is applied in the present study and is based on measurements of the sample impedance over a wide range of frequencies followed by analysis in the complex impedance plane. Results of the measurements can be used for determining an appropriate equivalent circuit of the system and for estimating the values of the circuit parameters.

The idea, how the conductivity of a sample can be estimated from the impedance analysis, will be described considering complex impedance diagram for various equivalent circuits of the sample (Xue et al., 2009). So, from the complex impedance measurements, one obtains in the complex impedance plane only one semicircle and this semicircle originates in the (0.0) point, it means that only one resistance R and one capacity C, both parallel combined, can be described to the sample. In such a case, these should be the bulk resistance and capacity of

the sample.

The dielectric properties of solid catalysts such as dielectric constant, dielectric loss factor and dielectric strength, usually determines the suitability of the catalyst material which may be considered as semi-conductor one (Lyon, 2010). The dielectric response results from the short range motion of charge carrier under the influence of magnetic field leading to storage of electrical energy and capacitance of the dielectric.

The present work aims to study a new behavior of mixed oxide catalysts which was found as semi-conductors in behavior which hoping to open a new field for development of catalysis.

EXPERIMENTAL AND RESULTS

Preparation Method

Nickel supported with Fe_2O_3 was promoted with nickel catalysts promoted with Fe_2O_3 and Supported with Al_2O_3, CoO and MnO, Al_2O_3, CoO and MnO additional promoters to obtain ternary mixed catalysts. They were prepared by Co- precipitation of calculated amounts of the corresponding nickel, ferric, aluminum, cobalt and manganese nitrate solutions by means of sodium carbonate solution at room temperature (Li et al., 2011). To ensure complete precipitation, one molar nitrate solutions of such elements were mixed together and added to about 1.5 molar solution of sodium carbonate under continuous mixing, the precipitate was then washed by breaking up the filter cake in a small amount of bi-distilled water and adding additional amount of about five liters bi-distilled water and stirring up the whole mass for one quarter 30 min. The washing cycle was repeated until the catalyst becomes free from impurities.

The obtained material was then dried for twenty four hours at about 105°C calcined at 350 - 370°C to decompose the metal carbonates into oxides, and then sieved into 0.2 - 0.4 mm diameters grains.

Reduction of the calcined material was then made using hydrogen gas at about 320°C. The hydrogen flow rate was about 15 L/h. The obtained catalyst was stabilized before use against spontaneous oxidation in air by impregnating in bi-distilled water and allowing slow oxidation to take place while heating up to 100°C. It is advisable to refresh the catalyst before use by passing hydrogen gas at a temperature of about 160°C for 2 h.

Conductimetric measurements

Conductivity measurements of the prepared ternary promoted nickel catalysts were calculated using a conductivity Bridge (Impedance Meter B.M. 507). The AC conductivity of solids is generally analyzed in terms of equivalent circuits composed of frequency independent resistors and capacitors. The AC response does not correspond to that predicated by simple idea circuits.

For instance semicircles in the complex impedance plane Z^* are often broadened and distorted in to symmetric arcs (Barczynski et al., 2010).

The powder catalyst samples were pressed into tablets under mechanical pressure of 10 tons/inch followed by coating with silver paste to be used as electrodes placed in muffel furnace calibrated with elevated temperature.

The conductivity bridge permits measuring of frequency (f) from 5 to 500 KHZ, impedance |Z| in KΩ and phase angle θ. From these measurements, it was possible to calculate both real resistance ($\bar{Z}_R$) and imaginary resistance ($\bar{\bar{Z}}_{Imagin}$) using the following equations;

$$\bar{Z}_{Real} = |Z| \cos \varnothing \quad (7)$$

$$\bar{\bar{Z}}_{Imagin} = |Z| \sin \varnothing \quad (8)$$

The relation between the real resistance ($\bar{Z}_{Real}$) and the imaginary one ($\bar{\bar{Z}}_{Imagin}$) gives a semi-circle starting from the origin and intercepts the $\bar{Z}_{Real}$ -axis in the bulk resistance (R_{bulk}). It was possible to estimate R_{bulk} -values at different temperatures ranging from 25 to 250°C. Accordingly conductivity values (σ) were calculated from the equation:

$$\sigma = \frac{1}{R_{bulk}} \cdot \frac{t}{A} \ \Omega.cm^{-1} \quad (9)$$

Where,
R_{bulk} is the catalyst-disc resistance (Ω),
A: is the area of the disc (cm^2),
t: is the disc thickness (cm).

The following equation correlates the AC conductivity with temperature;

$$\sigma = \sigma_o \, e^{-Ea/KT} \quad (10)$$

Where
Ea: is the activation energy,
K: is Boltzman's constant, and
T: is the absolute temperature.

Equation 10 permits calculation of the activation energy from the equivalent Arhenius Plots. In addition the dielectric constant (∈) of catalyst disc can be calculated from the following equation.

$$\in = \frac{C_x \ t}{\epsilon_o \ A} \quad (11)$$

Where;
t: is the thickness of the disc,
ϵ_o: is the permittivity of free space, (8.854 × 10^{-12} Farad/cm) ,
A: is the disc area.
C_x: is the capacitance and is given by:

$$C_x = \frac{1}{\omega \bar{\bar{z}}} = \frac{1}{2\Pi f \ \bar{\bar{z}}} \quad (12)$$

Where f: is the frequency

The experimental results are given in Table 1 and the $\bar{\bar{Z}}_{Imagin}$ versus $\bar{Z}_{Real}$ for the selected examined catalysts A5, B5 and C5 are represented in Figures 1 to 3.

From these results it was possible to calculate both conductivity and dielectric constant for the examined catalyst samples using the Equations 9 and 11. The results are given in Table 2.

Also, Table 3 summarizes the values of $\bar{\bar{Z}}_I$ frequency (f), capacitance (c_x) and dielectric constant (ϵ_r) for the examined catalytic systems.

Equation 10 was used to express the calculated a.c. conductivity values as a function of temperature. These results permitted calculation of the activation energy Ea.

The data were deduced front Arrhenius Plots relating log σ and $\frac{1}{T}$ for the different catalysts under investigation to produce Ea-values are given in Table 4.

Dielectric constant measurement

The calculation of dielectric constant (Taninouchi and Ichitsubo, 2010) of the selected ternary supported Nickel catalysts could be calculated using the equations:

$$\epsilon_r = \frac{c.d}{\epsilon_o A} \quad (13)$$

Where
C: The capacitance of the sample in Farad (F)
d: The thickness of the sample in meter (m)
A : The cross-sectional area of the parallel surface of the sample in m^2.
ϵ_o : The free space permittivity = 8.85 × 10^{-12} F/m.

The dielectic loss tangent (tan δ) was calculated from the phase angle (ϕ) using the formula:

tan (δ) = tan (90-ϕ) (14)

The A.C conductivity of the sample was calculated by the relation:

σ_{ac} = (t/A) I cos (15)

Where,
I: The current pass through the sample.
t: The thickness of the sample.
A: The cross-sectional area of the sample.
ϕ : The phase angle.
The A. C measurements have been carried out in the range of frequency from 50 Hz to 500 KHz.

DISCUSSION

The a.c. conductivity of the examined ternary promoted nickel catalysts using the complex impedance method produced semicircles permitting calculation of the electrical conductance of the samples under investigation at different temperatures.

It is clear from the measurements that the bulk conductivity of the catalysts has an electronic nature.

The conductivity is reffered to the motion of the charge carriers of the catalysts under investigations. Also, the dielectric properties in general, is treating the isolation of the material under considerable factors and is depending on frequency, temperature, and other factors which changes the properties of the catalyst itself. The dielectric constant reflects the internal structure of the material regarding the electronic and moleculer arrangments of the internal structure at elevated temperatures.

The application of an external electric field to a. dielectric solid induces a macroscopic polarization. For a real dielectric, the response of the catalyst is not instantaneous and therefore the polarization and the applied electric field are lagged in time, providing an interesting example- of relaxation process, the so called dielectric relaxation (Vaquero and Melendo, 2011).

Table 2 has the results of AC conductivity and Activation energy: The electrical properties of Ni/Fe_2O_3 oxides promoted with different metal oxides such as Al_2O_3, CoO and MnO depend largely on their structures, composition and method of preparation. At these polycrystalline materials the resistance of the metal oxides may be a combination of the bulk crystal resistance (R_b) and the grain boundary resistance (R_{gb}).

The bulk crystal resistance is in parallel with an associated bulk capacitance, in which the bulk resistance R_b is usually temperature dependent whereas capacitance changes a little with changing temperatures (El-Sayet et al., 2011; Sheng et al., 2011; Pingan et al., 2012).

The impedance diagrams at different temperature given in Figures 1, 2 and 3) show that the complex impedance method was found to form semi-circles passing through the origin. The semicircles are due to a parallel combination of the intragrain resistance R_b in which the

Table 1. Real resistance ($\bar{z}_R$) as a function of imaginary resistance ($\bar{\bar{z}}_I$) at different temperatures for ternary promoted Nickel catalysts.

25°C		50°C		100°C		150°C		200°C	
$\bar{z}_R$	$\bar{\bar{z}}_I$	$\bar{z}_R$	$\bar{\bar{z}}_I$	$\bar{z}_R$	$\bar{\bar{z}}_I$	$\bar{z}_R$	$\bar{\bar{z}}_I$	$\bar{z}_R$	$\bar{\bar{z}}_I$
Catalyst A5									
635.79	135.14	490.81	95.4	484.81	874.62	1791.84	4667.9	420-20	9396.93
579.56	155.29	440.17	93.56	268.78	700.19	1328.77	4089.54	338.97	7650.44
535.53	163.73	426.93	106.45	185.41	570.63	905.87	3380.74	572.49	6306.92
507.43	184.69	403.73	115.77	112.48	487.19	652.36	2825.67	781.42	4431.63
460.25	195.37	382.52	116.95	79.88	453.01	459.85	2365.72	531.88	3358.14
418.77	213.38	368.75	126.97	50.1	356.49	312.87	1975.38	248.78	2366.96
385.73	231.76	354.76	136.18	30.31	288.41 1	192.5	1568.22	125.26	1795.62
327.66	229.43	317.21	147.92	21.35	244.07	95.87	1095.81	65.42	1248.22
268.12	224.98	288.62	159.99	13.95	199.51	58.59	837.95	49.72	948.69
219.2	219.2	274.29	164.81	7.96	151.79	48.13	688.32	26.52	759.54
157.33	194.29	248.71	167.76	1.83	104.98	30.35	579.21	9.59	549.92
120.23	178.24	217.6	176.23	-	80	15.36	439.73	0	328
95.79	159.43	196.22	170.57	-	65	6.28	359.95	0	260
79.99	144.31	172.64	166.72	-	-	2.62	299.99	-	-
59.18	121.34	145.87	162.01	-	-	2.09	239.99	-	-
44.93	105.86	116.98	149.72	-	-	0	185	-	-
35,84	93.34	77.26	128.58	-	-	0	125	-	-
26.27	80.84	52.83	113.29	-	-	-	-	-	-
18.74	56.37	38.7	100.83						
9.35	48.09								
5.32	37.83								
3.32	31.62								
Catalyst B5									
5383.05	1543.57	4136.19	729.32	2756.37	9612.62	2298.26	9217.81	8571.67	5150.38
5068.42	1549.57	3926.51	763.24	1663. 2	7825.18	1215.54	6893.65	6582.18	6137.98
4755.28	1545, 09	3605.17	832.32	1007.3	5711.89	606.26	5768.22	5142.3	6128.36
4201.11	1612.66	3493.06	870.92	723.7	5149.39	479.23	4976,98	114.49	5663.12
3385.82	1725.16	3284.15	879.98.	322.48	3685.92	383.49	4383.26	935.72	4885.85
2883.36	1801.76	3380.74	905.87	261.17	2988.58	331.19	3785.54	253.46	4238.15
2053.72	1825.03	2966.99	1198.74	181.74	2593.67	251.07	3190.14	708.29	3836.89
1901.52	1977,79	2718.92	1267.85	149.98	2144.76	188.34	2693.42	26.06	2819.08
1636.79	1755,25	2424.87	1400	86.35	1647.74	116.14	2196.98	730.93	2390.76
1175.57	1618,03	2129.79	1491.29	39.44	1129.31	88.97	1697.67	606.4	2114.78
834.36	1388,61	1886.77	1640.15	34.89	799.24	41.18	1179.28	447.56	1795
547.96	1123.49	1697.06	1697.06	23.03	659.59	29.66	849.48	301.47	1418.31
374,61	927.18	1321.57	1632.01	19.54	559.66	24.43	699.57	182.33	1034.05
227.86	661.86	1062,47	1575.17	11.26	429.85	15.18	579.8	115.76	740.76
144.94	540.92	671.91	1318.69	6.11	349.95	7.68	439.93	89.07	633.77
116,60	467.63	430.04	1120.29	4.79	274.96	6.28	359.95	49.65	472.39
66.78	343.57	245.59	803,29	3.87	221.97	2.62	299.99	29.63	333.71
35.98	227.17	164.51	659.8	1.48	169.99	2.01	229.99	21.18	269,17
19.74	160.79	106.85	549.71	0	118	0	178	46.73	668.36
13.07	149.42	57.88	365.44			0	120	27.21	519.29
5.58	79.81	37.17	302.73					6.19	354.95
1.08	61.99	17.43	199.24					0	280
0.89	50.99	10.88	155.62					5	230

Table 1 Contd.

Catalyst C5									
675	133	480	90	400	800	1800	4600	3100	8000
579	155	430	90	270	690	1200	3800	2000	6700
516	157	420	104	180	560	900	3800	1500	6200
498	181	390	113	110	480	600	2700	700	3900
451	191	380	120	80	440	500	2400	500	3800
409	208	360	120	50	350	300	2000	200	2300
377	227	350	130	30	280	200	1500	100	1700
328	229	310	140	20	240	100	1100	100	1200
279	195	280	160	10	190	60	830	50	940
229	193	260	160	7	140	30	570	30	740
169	169	240	160	2	90	20	430	10	530
126	155	210	170	0	70	10	350	0	320
100	149	190	160	-	-	3	290	0	240
80	137	180	160	-	-	0	170	-	-
60	114	140	160	-	-	0	120	-	-
48	99	110	140						
35	83	70	120						
30	78	50	110						
21	64	40	110						
13	46								
7	36								
4	31								

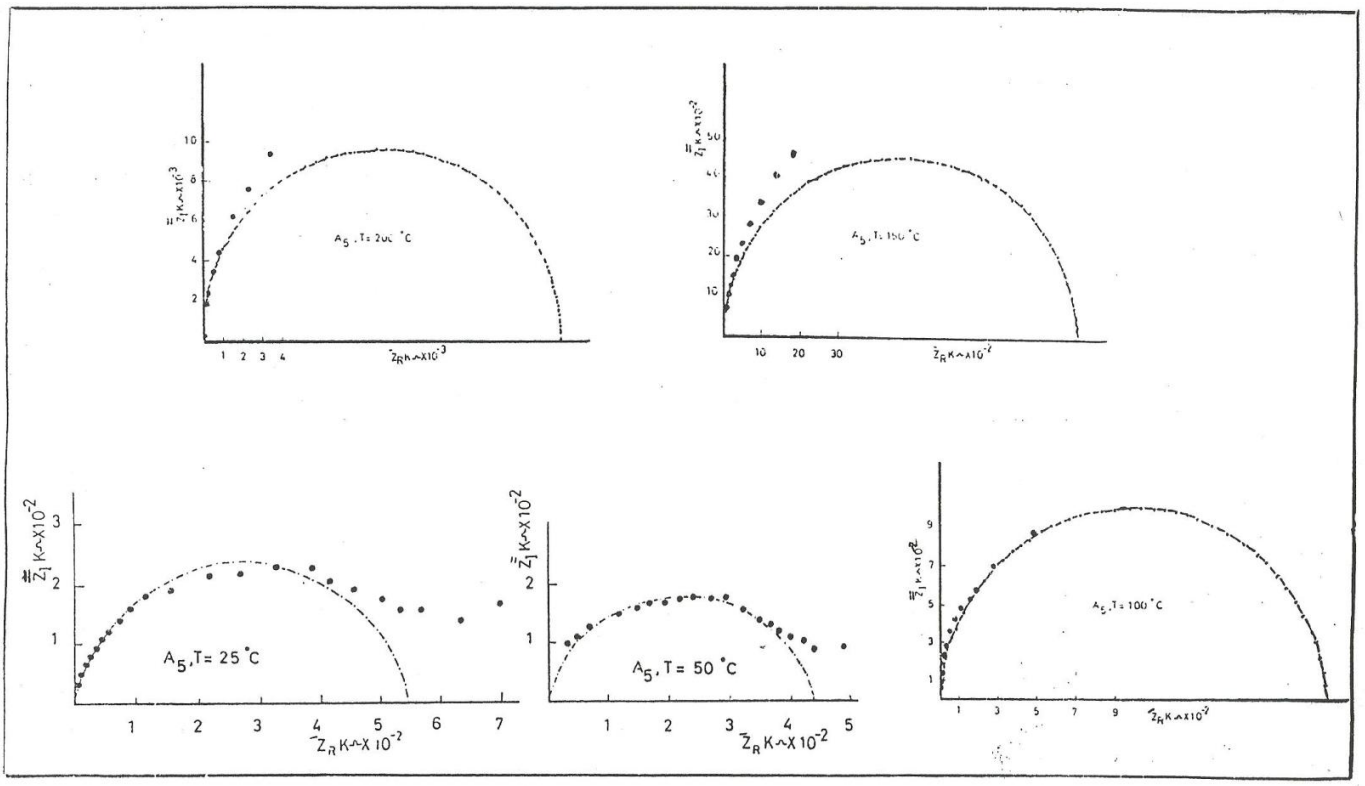

Figure 1. Typical complex impendence plots of catalyst A5 (85% Ni/10% Fe_2O_3/ 5% Al_2O_3).

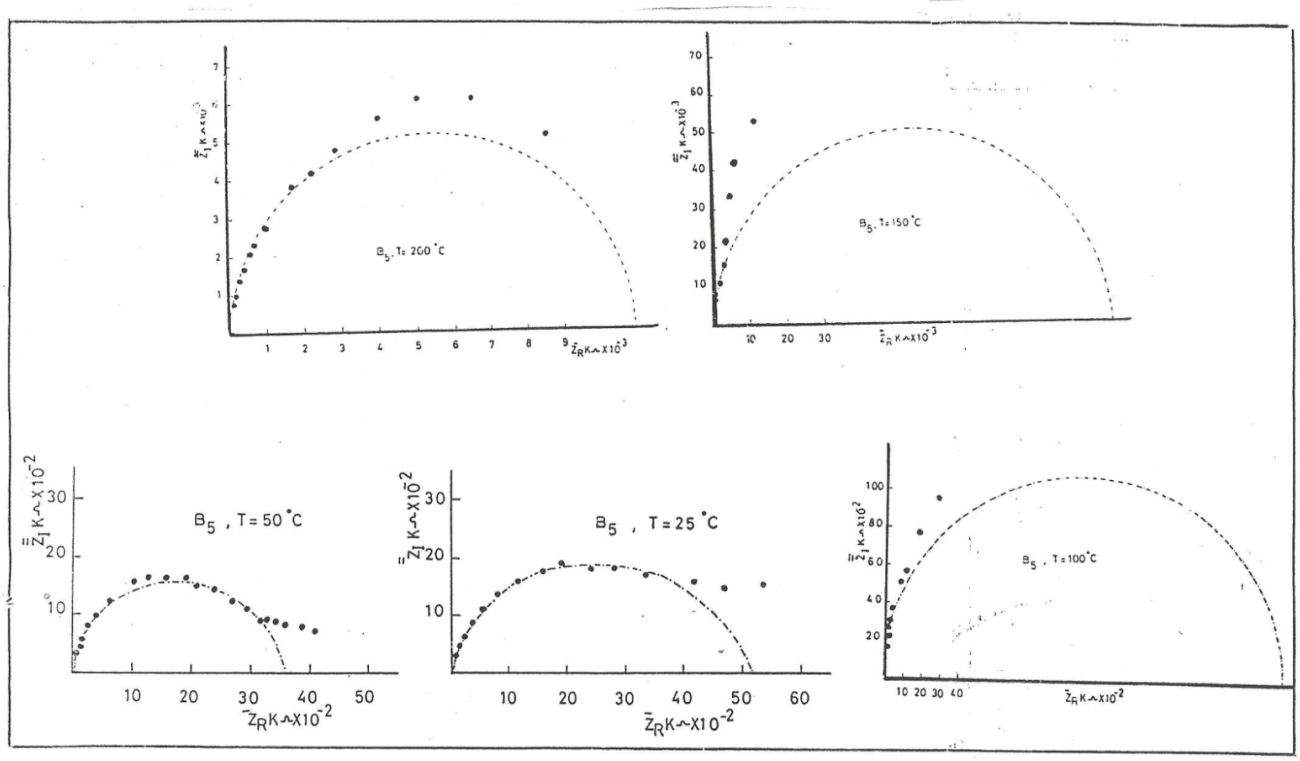

Figure 2. Typical complex impendence plots of catalyst B5 (85% Ni/10% Fe_2O_3 / 5% CoO).

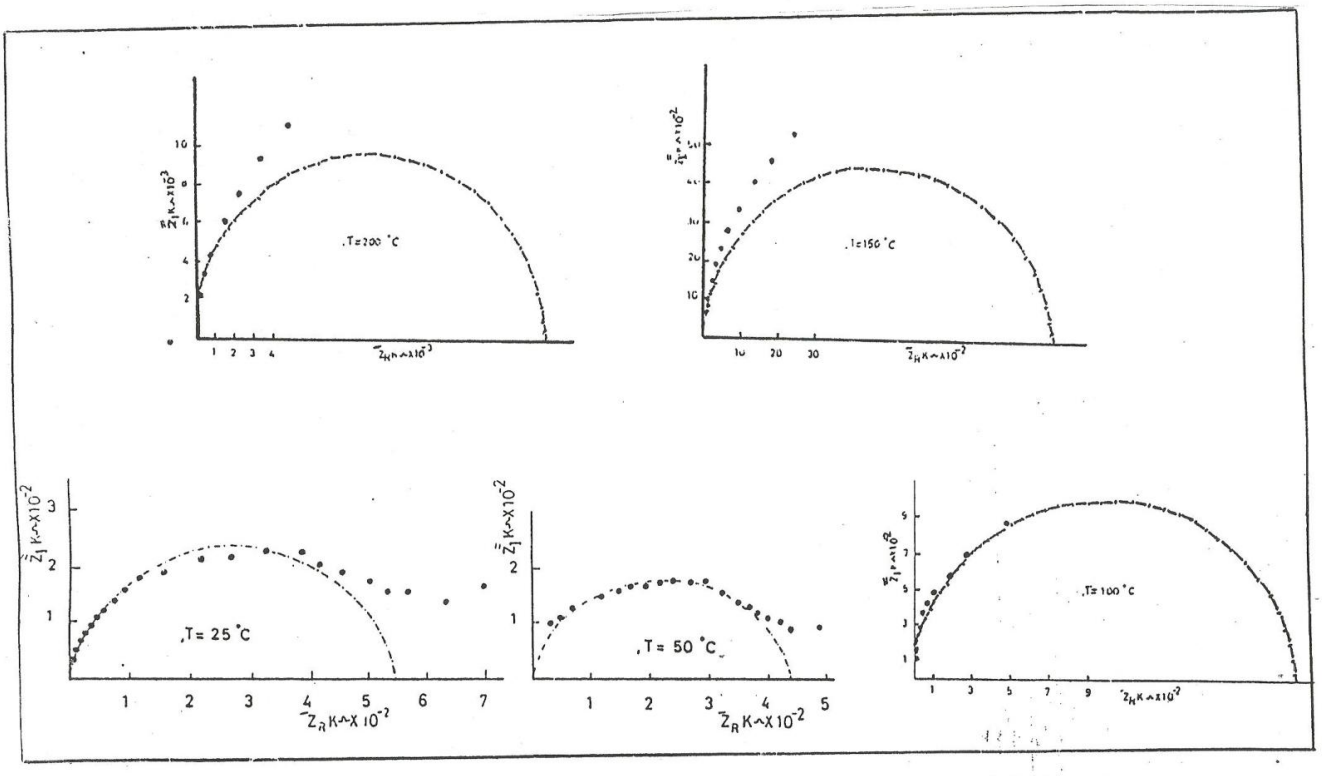

Figure 3. Typical complex impendence plots of catalyst C5 (85% Ni/10% Fe_2O_3 / 5% MnO).

Table 2. Resistance (R) conductance (δ) and activation energy (Ea) for selected catalysts.

Catalyst	Temp. °C	RΩ	δΩ/cm	$Ea_{e.v}$
	25	55	7.4×10^{-4}	
A5	50	44	9.3×10^{-4}	
$Ni/Fe_2O_3/Al_2O_3$	100	200	2×10^{-4}	0.4
85%/10%/5%	150	920	4.4×10^{-4}	
	200	185	2.2×10^{-4}	
	25	520	2.4×10^{-4}	
B5	50	300	4.1×10^{-4}	0.5
$Ni/Fe_2O_3/CoO$	100	2150	5.7×10^{-4}	
85%/10%/5%	150	107	1.1×10^{-4}	
	200	11	0.0111	
	25	590	6.9×10^{-4}	
C5	50	480	8.5×10^{-4}	
$Ni/Fe_2O_3/MnO$	100	890	4.6×10^{-4}	0.1
85%/10%/5%	150	1001	4.1×10^{-4}	
	200	1000	4×10^{-4}	

Table 3. Imaginary Resistance $\bar{Z}_I$, Frequency ('f), Capacitance (C_x) and Dielectric Constant ($\in_r$) for Ternary Promoted Nickel Catalysts.

Catalyst A5 (25°C)					
$''Z_1$	f KHz	W (2πf)	C_x x10^{-5}	$\in_r$ x10^{-6}	Log F
135.14	0.5	3.142	2360	1090	-0.30
155.29	1.2	7.539	854	394	0.08
163.73	2	12.566	486	224	0.30
184.69	3	18.849	287	132	0.50
195.73	4	25.133	204	94.0	0.60
213.38	5	31.416	149	88.9	0.70
231.76	7	43.982	98.10	45.2	0.80
229.43	10	62.832	69.40	31.9	1.00
224.98	15	94.248	47.20	21.8	1.20
219.20	20	125.664	36.30	16.7	1.30
194.29	30	188.496	27.30	12.5	1.50
178.28	40	251.327	22.30	10.3	1.60
159.43	50	314.159	19.90	9.17	1.70
144.31	60	376.991	18.40	9.47	1.80
121.34	80	502.655	16.40	7.56	1.90
105.89	100	628.319	15.00	6.91	2.00
93.34	120	753.982	14.20	6.54	2.10
80.84	150	942.478	13.10	6.03	2.20
56.37	200	1256.640	14.10	6.49	2.30
48.09	300	1884.960	11.00	5.07	2.50
37.83	400	2513.270	10.50	4.84	2.60
31.62	500	3141.560	10.01	4.65	2.70
Catalyst A5 (50°C)					
95.40	2	12.57	834	384	0.3

Table 2 Contd.

93.60	4	25.13	405	196	0.6
106.45	5	31.42	299	137	0.7
115.77	10	62.83	137	63.1	1.0
116.95	12	75.39	113	52.1	1.1
126.97	15	94.25	83.50	38.5	1.2
136.18	20	125.66	58.40	26.9	1.3
147.92	30	188.94	35.90	16.5	1.5
159.99	40	251.33	24.90	11.5	1.6
164.81	50	314.16	19.30	8.89	1.7
167.79	60	376.99	15.90	7.28	1.8
176.21	80	502.66	11.30	5.21	1.9
170.57	100	628.32	9.33	4.29	2.0
166.72	120	753.98	7.96	3.66	2.1
162.01	150	942.48	6.55	3.02	2.2
149.72	200	1256.64	5.32	2.45	2.3
128.58	300	1884.96	4.13	1.90	2.5
113.29	400	2513.27	3.51	1.62	2.6
100.83	500	3141.59	3.16	1.46	2.7
		Catalyst A5 (100°C)			
874.63	20	125.66	9.09	4.18	1.3
700.19	30	188.49	7.58	3.48	1.5
570.63	40	251.33	6.97	3.21	1.6
487.19	50	314.16	6.53	3.00	1.7
453.01	60	376.99	5.96	2.69	1.8
356.49	80	502.66	5.51	2.54	1.9
288.41	100	628.32	5.52	2.54	2.0
244.07	120	753.98	5.43	2.50	2.1
199.51	150	942.48	5.32	2.44	2.2
151.79	200	1256.64	5.24	2.41	2.3
104.98	300	1884.96	5.05	2.33	2.5
80.00	400	2513.27	4.97	2.29	2.6
65.00	500	3141.59	4.89	2.25	2.7
		Catalyst A5 (150°C)			
4667.90	5	31.42	6.82	3.14	0.7
4089.90	6	37.69	6.49	2.98	0.8
3380.74	8	50.27	5.88	2.71	0.9
2825.67	10	62.83	5.63	2.59	1.0
2365.72	12	75.39	5.61	2.58	1.1
1975.38	15	94.25	5.37	2.47	1.2
1568.22	20	125.66	5.07	2.33	1.3
1095.81	30	188.94	4.84	2.23	1.5
837.95	40	251.33	4.75	2.19	1.6
688.32	50	314.16	4.62	2.13	1.7
579.21	60	376.99	4.58	2.11	1.8
439.73	80	502.66	4.52	2.08	1.9
359.95	100	628.32	4.42	2.03	2.0
299.99	120	753.98	4.42	2.03	2.1
239.99	150	942.48	4.42	2.03	2.2
185.00	200	1256.64	4.30	1.98	2.3

Table 2 Contd.

125.00	300	1884.96	4.24	1.97	2.5
Catalyst A5 (200°C)					
9396.93	3	18.85	5.65	2.60	0.5
7650.44	4	25.13	5.20	2.39	0.6
6306.92	5	31.42	5.05	2.33	0.7
4431.63	7.5	47.12	4.79	2.21	0.9
3358.14	10	62.83	4.77	2.19	1.0
2366.96	15	94.25	4.48	2.06	1.2
1795.62	20	125.66	4.43	2.03	1.3
1248.89	30	188.49	4.25	1.96	1.5
948.69	40	251.33	4.19	1.93	1.6
759.54	50	314.16	4.19	1.92	1.7
549.92	70	439.82	4.13	1.90	1.8
328.00	120	753.98	4.04	1.86	2.1
260.00	150	942.48	4.08	1.86	2.2
Catalyst B5 (25°C)					
1543.57	0.12	0.75	880	1190	-0.9
1549.57	0.20	1.26	520	720	-0.7
1545.09	0.30	1.88	340	470	-0.5
1612.66	0.50	3.14	197	270	-0.3
1725.16	1.2	7.54	77	110	0.1
1801.96	2	12.57	44	61	0.3
1825.03	3	18.85	29	40	0.5
1977.79	4	25.13	20	30	0.6
1755.25	5	31.42	18	20	0.7
1618.03	7	43.98	14	19	0.8
1388.61	10	62.83	11	15	1.0
1123.49	15	94.25	9	12	1.2
927.18	20	125.66	8.5	12	1.3
661.86	30	133.49	8.0	11	1.5
540.92	40	251.33	7.3	10	1.6
467.88	50	314.15	6.8	9.4	1.7
343.57	70	439.82	6.6	9.1	1.8
227.17	100	628.32	6.4	8.8	2.0
160.79	150	942.48	6.6	9.1	2.2
149.42	200	1256.63	5.3	7.3	2.3
79.81	300	1884.96	6.6	9.1	1.5
61.99	400	2513.27	6.4	8.8	2.6
5099	500	3141.59	6.3	8.7	2.7
Catalyst B5 (50°C)					
729.32	0.06	0.38	3600	4900	-1.2
763.24	0.10	0.63	2100	2900	-1.0
832.32	0.20	1.26	950	1300	-0.7
870.92	0.30	1.88	610	240	-0.5
879.98	0.40	2.51	450	620	-0.4
905.87	0.50	3.14	350	480	-0.3
1198.74	1.5	9.42	39	120	0.18
1267.85	2	12.57	63	87	0.3

Table 2 Contd.

1400.00	3	18.85	38	52	0.5
1491.24	4	25.13	27	36	0.6
1640.15	5	31.42	19	26	0.7
1697.06	6	37.69	16	22	0.8
1632.01	8	50.27	12	16	0.9
1576.17	10	62.83	10	13	1.0
1318.69	15	94.25	8	11	1.2
112.29	20	215.66	7.1	9.8	1.3
803.29	30	188.94	6.6	9.1	1.5
659.80	40	251.33	6.1	8.2	1.6
549.71	50	314.15	5.8	8.0	1.7
365.44	80	502.65	5.4	7.4	1.9
302.73	100	628.32	5.3	7.2	2.0
199.24	150	942.48	5.3	7.3	2.2
155.62	200	1256.64	5.1	7.0	2.3
107.98	300	1884.96	4.9	6.7	2.5
76.99	400	2513.27	5.2	7.1	2.6
62.99	500	3141.25	5.1	7.0	2.7
		Catalyst B5 (100°C)			
9612.62	2.1	13.19	7.9	11.00	0.3
7825.18	3	18.85	6.8	9.4	0.5
5711.98	4	25.13	6.9	9.5	0.6
5149.59	5	31.42	6.2	8.50	0.7
3658.92	8	50.27	5.4	7.45	0.9
2988.58	10	62.83	5.3	7.32	1.0
2593.67	12	75.39	5.1	7.00	1.1
2144.78	15	94.25	4.9	6.91	1.2
1647.74	20	125.66	4.8	6.60	1.4
1129.31	30	188.94	4.7	6.48	1.5
799.24	40	251.33	4.9	6.76	1.6
659.59	50	314.15	4.8	6.62	1.7
559.66	60	376.99	4.7	6.48	1.8
429.85	80	502.65	4.6	6.30	1.9
349.95	100	628.32	4.5	6.21	2.0
274.96	120	753.98	4.8	6.62	2.1
221.97	150	942.48	4.8	6.62	2.2
196.99	200	1256.63	4.7	6.48	2.3
118.00	300	1884.96	4.51	6.21	2.5
		Catalyst B5 (150°C)			
9217.81	2.5	15.71	6.9	9.5	0.4
6893.65	4	25.13	5.7	7.8	0.6
5768.22	5	31.42	5.5	7.6	0.7
4976.98	6	37.69	5.3	7.3	0.8
4383.86	7	43.98	5.2	7.2	0.8
3785.54	8	5.027	5.3	7.3	0.9
3190.14	10	62.83	5.0	6.9	1.0
2693.42	12	75.39	4.9	6.8	1.1
2196.98	15	94.25	4.8	6.6	1.2
1697.67	20	125.66	4.7	6.4	1.3
1179.28	30	188.94	4.5	6.2	1.5

Table 2 Contd.

849.48	40	251.33	4.7	6.5	1.6
699.59	50	314.15	45.5	6.3	1.7
579.80	60	376.99	4.6	6.4	1.8
4390.93	80	502.65	4.5	6.2	1.9
359.95	100	628.32	4.4	6.1	2.0
299.99	120	753.98	4.4	6.1	2.1
229.99	150	942.48	4.6	6.4	2.2
178.00	200	1256.63	4.5	6.2	2.3
120.00	300	1884.96	4.4	6.1	2.5
		Catalyst B5 (200°C)			
5150.38	0.9	5.65	3.4	47.0	0.04
6137.98	1.2	7.54	2.2	30.0	0.08
6128.36	1.5	9.42	1.7	23.0	0.18
5663.12	2	12.57	1.4	19.0	0.3
4885.85	3	18.85	1.1	15.0	0.5
4238.15	4	25.13	9.4	13.0	0.6
3836.89	5	31.42	8.3	12.0	0.7
2819.08	8	50.27	7.1	9.8	0.9
2390.76	10	62.83	6.7	9.2	1.0
2114.78	12	75.39	6.3	8.0	1.1
1795.0	15	94.25	5.9	7.7	1.2
1418.31	20	125.66	5.6	7.0	1.3
1034.05	30	188.94	5.1	7.5	1.5
740.76	40	251.33	5.4	6.9	1.6
633.77	50	314.15	5.1	6.9	1.7
472.39	70	439.82	4.8	6.6	1.8
338.71	100	628.32	4.7	6.8	2.0
269.17	120	753.98	4.9	6.7	2.1
668.36	150	942.48	1.6	2.2	2.2
519.29	200	1256.64	1.5	2.1	2.3
354.95	300	1884.96	1.5	2.9	2.5
280.00	400	2513.27	1.4	1.7	2.6
230.00	500	3141.59	1.4	1.8	2.2
		Catalyst C5 (25°C)			
F_{KHz}	**$\bar{\bar{Z}}$**	**W ($2\pi f$)**	**C_x x10^{-6}**	**ϵ_r x10^{-6}**	**Log F**
0.5	133	3.14	2390	1100	-0.3
1.2	155	7.54	856	390	0.08
2.0	157	12.56	425	210	0.30
3.0	181	18.85	293	130	0.5
4.0	191	25.13	208	96	0.6
5.0	208	31.42	153	70	0.7
7.0	227	43.98	100	46	0.8
10.0	229	62.93	69.5	32	1.0
15.0	195	94.25	56.7	26	1.2
20.0	193	125.66	57.2	26	1.3
30.0	169	188.49	31.4	14	1.5
40.0	155	251.33	25.7	12	1.6
50.0	149	314.10	21.4	9.9	1.7
60.0	137	376.99	19.4	8.9	0.8

Table 2 Contd.

80.0	114	502.65	17.5	8.1	0.9
100.0	99	628.32	16.1	7.4	2.0
120.0	83	753.98	15.9	7.3	2.1
150.0	78	942.48	13.6	6.3	2.2
200.0	64	1256.64	12.4	5.7	2.3
300.0	4	1884.96	11.5	5.3	2.5
400.0	36	2513.27	11.0	5.1	2.6
500.0	31	3141.59	10.0	4.6	2.7
Catalyst C5 (50°C)					
2	90	12.57	880	410	0.3
4	90	25.13	440	200	0.6
5	104	31.42	310	140	0.7
10	113	62.83	140	64	1.0
12	120	75.39	110	51	1.1
15	120	94.25	88	41	1.4
20	130	125.66	61	28	1.3
30	140	188.49	38	17	1.5
40	160	251.33	25	12	1.6
50	160	314.16	19	8.7	1.7
60	160	376.99	17	7.8	1.8
80	170	502.65	12	5.5	1.9
100	160	628.32	9.0	4.5	2.0
120	160	753.98	8.3	3.8	2.1
150	160	942.48	6.5	3.0	2.2
200	140	1256.64	5.7	2.6	2.3
300	120	1884.96	4.4	2.0	2.5
400	110	2513.27	3.6	1.7	2.6
500	100	3141.59	3.2	1.5	2.7
Catalyst C5 (100°C)					
20	800	125.66	9.9	4.6	1.3
30	690	188.49	7.7	3.5	1.5
40	560	251.33	7.1	3.3	1.6
50	480	314.16	6.6	3.0	1.7
60	440	376.99	6.0	2.8	1.8
80	350	502.67	5.7	2.6	1.9
100	280	628.32	5.7	2.6	2.0
120	240	753.98	5.5	2.5	2.1
150	190	942.48	5.6	2.6	2.2
200	140	1256.64	5.7	2.6	2.3
300	90	1884.96	5.9	2.7	2.5
400	70	3141.59	5.7	2.6	2.6
-	-	-	-	-	2.7
Catalyst C5 (150°C)					
5	4600	31.42	6.90	3.20	0.7
6	3800	37.69	6.90	3.10	0.8
8	3300	50.26	6.00	2.80	0.9
10	2700	62.83	5.90	2.70	1.0
12	2400	75.39	5.50	2.50	1.1

Table 2 Contd.

15	2000	94.25	5.30	2.40	1.2
20	1500	125.66	6.30	2.40	1.3
30	1100	188.49	4.80	2.20	1.5
40	830	251.33	4.80	2.20	1.6
50	570	314.16	5.60	2.60	1.7
60	430	376.99	6.20	2.90	1.8
80	350	502.65	5.70	2.60	1.9
100	290	628.32	5.50	2.50	2.0
120	170	753.98	7.80	2.40	2.1
Catalyst C5 (200°C)					
3	8000	18.85	6.60	3.00	0.5
4	6700	25.13	5.90	2.70	0.6
5	6200	31.42	5.10	2.30	0.7
7.5	3900	47.12	5.40	2.50	0.9
10	3300	62.83	4.80	2.20	1.0
15	2300	94.25	4.60	2.10	1.2
20	1700	125.68	4.70	2.20	1.3
30	1200	188.49	4.40	2.00	1.5
40	940	251.33	4.20	1.90	1.6
50	740	314.16	4.30	1.97	1.7
70	530	439.82	4.30	2.00	1.8
120	320	753.98	4.10	1.90	2.1
150	240	942.48	4.40	2.00	2.2

Table 4. The Arrhenius plots relating log δ and $\frac{1}{T}$ for the selected catalysts.

Catalyst	Log δ	$\frac{1}{T}$
A5	-3.19	3.35
	-3.02	3.09
	-3.70	2.68
	-4.37	2.36
	-3.66	2.11
B5	-3.61	3.35
	-3.41	3.09
	-4.3	2.68
	-2.93	2.36
	-1.95	2.11
C5	-3.17	3.35
	-3.08	3.09
	-3.30	2.68
	-4.40	2.36
	-4.43	2.11

value of intragrain intersepts the $\bar{Z}$-axis where $\bar{\bar{Z}}$ is zero. Also the temperature dependance of resistivity is analysed on the basis of the effective mean free path model (Brent et al., 2012; Lu et al., 2012).

The variation of log σ against $\frac{1}{T}$ for Ni/Fe_2O_3 supported with different metal oxides such as Al_2O_3, CoO and

MnO shows that the resistance increase with decreasing the temperature linearly, indicating an activated conduction and semiconductor nature.

The decrease of resistance during the heating may be attributed to the intrinsic conduction due to the presence of different metal oxides.

The activation energies calculated from these slopes vary from 0.11eV (it is written as found) to 0.5 eV, but most of these are nearly the same as can also be seen from the near parallelism of plots.

REFERENCES

Barczynski RJ, Krol P, Murawski L (2010). AC and DC conductivities in V2O5-P2O5 glasses containing alkaline. J. Non Cryst. Solids, 37-40, Vol. 356(37-40) pp. 1965-1967.

Brent T, Romano C, Genova D, Behrens H, Scariato P (2012). Mixed electrical conduction in a hydrous pantellerite glass. Chemical Geology. Vol. 320(321). pp 140-146

El-Sayet AM, Ismail FM, Yakout SM (2011). Electrical conductivity and sensitive characteristict of Ag-added BaTiO3-CuO mixed oxide for CO2 gas sensing. J. Mater. Sci. and Technol. Vol. 27(1). 35-40.

Gouda GM, Nagendro CL (2009). Structural and electrical properties of mixed oxides of manganese and vanadium, A new semiconductor oxide thermistor material. Sensors and Actuators A. Physical. Vol. 155: 263-271.

Lu H, L. Zhu, J. Kim, S. H. Son (2012). Structural,reduction-tolerant,sintering, and electrical properties. Solid State Ionics. Vol. 209: 24-29.

Lyon SB (2010). Corrosion of carbon and Low Alloy Steels, Vol. 3: 1693-1736.

Moseley PT (2009). Electrolytes solid,Sodium ion, Encylopedia of Eledtrochmical Power Sources. Pp. 196-214.

Pingan C, Luo G, Shen Q, Li M, Zhang L (2013). Thermaland electrical properties of W-Cu Composite produced by activated sintering. Materials and Design. Vol. 46: pp 101-105.

Sheng M, Donald RC, Yang H, Carios F, Willam R, Yantz J, Daniel K, Bruce J (2013) Effective thermal conductivity and junction factor for sintered microfibrous materials. Int. J. Heat Mass Transf. Vol. 56(1-2), pp 10-19.

Smallman RE, Ngan AHW (2007). Physical Metallurgy and Advanced Materials Engineering, Seventh Edition pp. 37-94.

Taninouchi YK, Ichitsubo T (2010). High oxide-ion conductivity of monovalent-metal-doped bismuth vanadate at intermediate temperatures).Solid State Ionics. Vol. 181(15-16) pp. 719-723.

Vaquero C, Melendo MJ (2011). Characterization and Creep Properties of Proton-Conducting Yb-doped barium cerate. J. Eur. Ceram. Soc., Vol. 31(14). 2671-2676, 2011.

Xue L, Zhao H, Xu N, Chen N (2009). Electrical conduction behavior of La,Co doped SrTiO3 perovskite as anode material for solid oxide fuel celles. Int. J. hydrogen Energy, Vol. 34(15) pp. 6407-6414.